arXiv:cond-mat/0307374v1 [cond-mat.supr-con] 15 Jul 2003

Do Vortices Entangle?

C.J. Olson Reichhardt and M. B. Hastings
Center for Nonlinear Studies and Theoretical Division, Los Alamos National Laboratory, Los Alamos, New Mexico 87545
(February 2, 2008)

We propose an experiment for directly constructing and locally probing topologically entangled states of superconducting vortices which can be performed with present-day technology. Calculations using an elastic string vortex model indicate that as the pitch (the winding angle divided by the vertical distance) increases, the vortices approach each other. At values of the pitch higher than a maximum value the entangled state becomes unstable to collapse via a singularity of the model. We provide predicted experimental signatures for both vortex entanglement and vortex cutting. The local probe we propose can also be used to explore a wide range of other quantities.

PACS: 74.25.Qt, 74.25.Sv

The high superconducting transition temperatures of compounds such as $YBa_2Cu_3O_{(7-\delta)}$ (YBCO) and $BiSr_2Ca_2CuO_8$ (BSCCO) lead to a very rich set of behaviors of the magnetic vortices which form inside the material in the presence of an applied magnetic field. Thermal fluctuations are significant over a wide range of the (H,T) phase diagram [1], causing the lattice of stiff vortex lines to melt well below T_c. The nature of this molten state has remained a subject of intense debate.

Since there can be significant thermally-induced wiggling along the length of the vortex in the liquid state, Nelson proposed that neighboring vortex lines may become entangled with each other, in analogy with a superfluidity transition in a boson system [2]. This entanglement could produce a dramatic increase in the viscosity of the vortex liquid [3–5], similar to that which occurs for entangled polymers. As a result, vortex pinning by random disorder in the sample would be enhanced, so that the resistivity would drop in the entangled state.

In order for the vortices to entangle, it is crucial that neighboring lines not cut through each other easily [6] and reconnect into a disentangled state. Estimates of the cutting barrier vary widely [3,5,7–10], ranging from $50k_BT$ to of order k_BT, leaving the question of whether vortices can easily cut in the liquid state unresolved. Numerical simulations performed in limits ranging from the low-field London regime to the high-field lowest Landau level regime have proven similarly ambiguous, with some simulations interpreted as providing evidence for entanglement [11] and others interpreted as showing that the lines cut and do not entangle [9,12,13]. The simulations are limited both by the models chosen and by the system sizes that can be simulated. Models based on the boson analogy lack long-range interactions along the vortex line, which can stiffen the vortices and might reduce entanglement. [7,14,15]. In the frustrated 3D XY model, there are multiple ways to define a path followed by a vortex line, some of which are consistent with entanglement, and others which are not [12].

Since theoretical and numerical evidence for entanglement have proven inconclusive up to this point, it is natural to turn to experiments to resolve the issue. Unfortunately experimental evidence for or against entanglement [16–19] has also proven ambiguous, both because the experimental measures are indirect, and because there is considerable variation in the definition of entanglement [20], such as equating entanglement with the onset of plasticity [16]. Thus, despite more than a decade of theoretical, numerical, and experimental studies, the question of whether vortices in high-temperature superconductors can form an entangled state has not yet been convincingly answered.

Here we propose a direct experimental test of vortex entanglement by means of a local atomic-force microscope (AFM) probe which can unambiguously determine whether it is possible for two vortices to wind around each other without cutting. We consider conditions that are as favorable as possible for entanglement: low vortex density, weak background pinning, and low temperatures, which should increase the barrier to flux cutting. We propose using a magnetic AFM tip to produce the simplest possible entangled state, two vortices wound around each other, and show theoretically that the forces involved in creating the entangled state can be measured with current technology. Should the vortices cut rather than entangling, a distinct force signature will be observed. If entanglement does not occur in this limit, it seems unlikely to occur in the higher density, higher temperature conditions near the melting transition. In addition to testing entanglement, the local AFM probe which we propose can be used to measure a wide range of other quantities, such as vortex line tension, local pinning force, and local shear forces.

We use as our definition of an entangled vortex state the picture originally proposed by Nelson, in which vortices behave like elastic lines that cannot easily cut through each other [2]. We consider a layered superconductor containing two closely spaced magnetic dots at the bottom of the sample [21] (dark circles in Fig. 1) A mobile magnetic dot is introduced to the top of the sample in the form of a magnetic AFM tip (open circle in Fig. 1). An optional additional magnetic dot

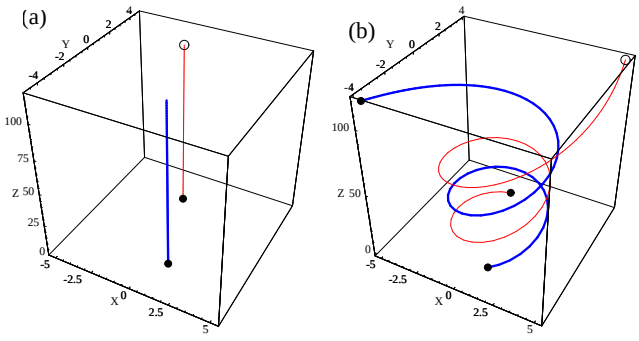

FIG. 1. (a) Schematic of the starting state. Black dots represent the fixed pins; the open circle represents the end of the vortex being moved by the AFM. (b) A configuration of wound vortices, found numerically by minimizing the free energy within an elastic string model. The lengths are in units of λ and the system is isotropic.

can be added at the top of the sample to pin one of the vortices. We assume that there is a sufficiently small externally applied magnetic field that there are only two vortex lines within the region of interest, an area a few λ on a side, where λ is the London penetration depth of the material. The magnetic dots attract the vortices, so that the top and bottom positions of the vortices are fixed at the dot locations. As the AFM is moved along the surface of the sample, it drags the top of one vortex. The force required to drag the vortex line can be directly measured. When the AFM tip moves in a circular path around the fixed upper dot, the two vortices wind together, producing an entangled state. In Fig. 1(b), we illustrate one possible entangled vortex configuration, obtained numerically as described below. As the winding angle increases, the force required to drag the vortex further around increases according to a form derived below. If the vortices cut, this force will abruptly drop. Thus, using such an experiment, it is possible to directly probe whether vortex entanglement can occur.

To estimate the force required to entangle a pair of linelike vortices, we represent the vortex lines as one-dimensional elastic strings that cannot cross. Such a model may be applicable in the London limit at low fields $B < 0.2B_{c2}$, although the lack of long-range interactions along the z axis is a notable limitation [7,14,15]. The vortex configuration is determined by a balance of the interaction energy, which drives the strings apart, and the elastic energy, which pulls the strings together to reduce their length as they are wound. Thus, the greater the pitch (defined as the rate of change of winding angle per vertical distance), the closer the vortices approach, as they seek the preferred spacing that minimizes their free energy. Even if they are held radially away from the preferred spacing, as is shown at the top of Fig. 1(b), they approach the preferred spacing within the middle of the sample, leading to the roughly constant spacing in the middle of the sample as shown. This applies up to a certain pitch; beyond that pitch, we will show that the vortices are unstable to a collapse. A similar instability in a related model was discussed in Ref. [8]. The existence within the model of a collapse of the entangled state at a singularity when the vortices approach each other too closely raises the question of whether the entangled state can exist in other experimental situations where the vortices are driven closer than this distance.

Elastic String Model— We consider two vortices, at positions $\vec{r}_1(z), \vec{r}_2(z)$, with $\vec{r} = (x, y)$, giving the position in the plane as a function of the vertical distance z. As a starting point, we consider the free energy from the elastic string model [3]:

$$F = \int_0^L \mathrm{d}z \sum_i \frac{1}{2}\tilde{\epsilon}_1(\partial_z \vec{r}_i)^2 + 2\sum_{i<j} \epsilon_0 K_0(|\vec{r}_i(z) - \vec{r}_j(z)|/\lambda), \tag{1}$$

with $\epsilon_0 = (\Phi_0/4\pi\lambda)^2$, $\tilde{\epsilon}_1 \approx \sqrt{M_\perp/M_z}\epsilon_0$. We fix the boundary conditions on the vortex position at the top ($z = L$) and the bottom ($z = 0$) of the sample, and then minimize the free energy (1) to find the positions of the vortex in between. To specify these positions, we need eight real numbers, two for each vortex at the top and another two for each vortex at the bottom. To simplify, let us fix two of these coordinates by setting $\vec{r}_1(0) + \vec{r}_2(0) = 0$; thus, the origin of the coordinate system is set at the midpoint of the two vortices at the bottom of the sample.

We note that if a given pair of functions $\vec{r}_{1,2}(z)$ minimize the free energy for given boundary conditions $\vec{r}_{1,2}(L)$, then the functions $\vec{r}_{1,2}(z) + \vec{v}z$ also minimize the free energy for a different set of boundary conditions: $\vec{r}_{1,2}(L) + \vec{v}L$. Thus, it suffices to consider only the case in which also $\vec{r}_1(L) + \vec{r}_2(L) = 0$, as then all other boundary conditions at the top can also be obtained. In this case, for all z, $r_1(z) + r_2(z) = 0$. Thus, introduce coordinates with $r_1(z) = [r(z)\cos(\theta(z)), r(z)\sin(\theta(z))]$ and $r_2(z) = -r_1(z)$. For the boundary conditions, we fix $r(0), r(L), \theta(0), \theta(L)$. Then, the extremization of the free energy yields equations of motion:

$$r^2\theta_z = J \tag{2}$$

$$\tilde{\epsilon}_1(\partial_z^2 r - J^2/r^3) + (2\epsilon_0)K_1(2r/\lambda)/\lambda = 0. \tag{3}$$

Exploiting an analogy of this system to a particle evolving in time, the first equation is the familiar conservation of angular momentum.

There exist solutions with constant vortex spacing, $r(z)$, and pitch, $\partial_z\theta(z)$. To find these, set $\partial_z^2 r = 0$ in the equations of motion to obtain

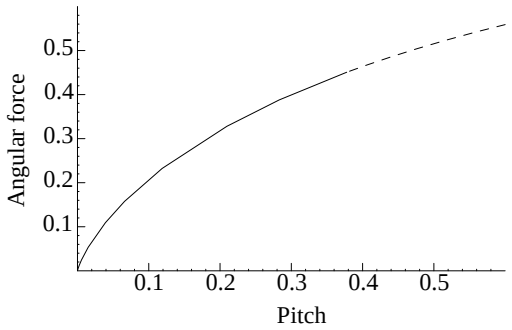

FIG. 2. Angular force on the top end of each vortex as a function of pitch $\partial_z\theta$. Force is measured in units of $\tilde{\epsilon}_1$, pitch in units of $\sqrt{\epsilon_0/\tilde{\epsilon}_1}/\lambda$. The dashed line denotes an unstable vortex configuration above a pitch of approximately 0.378, corresponding to a closest vortex spacing of $r \approx 1.19\lambda$.

$$\partial_z\theta = \sqrt{\frac{K_1(2r/\lambda)}{r\lambda}\frac{2\epsilon_0}{\tilde{\epsilon}_1}}. \tag{4}$$

This gives the preferred pitch as a function of spacing, by a balance between elastic energy of one vortex and interaction energy between two. For small r, this reduces to $\partial_z\theta = (1/r)\sqrt{\epsilon_0/\tilde{\epsilon}_1}$. From this one can show that for small spacing in the isotropic system ($\epsilon_0 = \tilde{\epsilon}_1$) the vortices cross at an angle of $\pi/2$, as expected [8]. While this scenario seems reasonable, we will find later that there is a major caveat: Eq. (4) describes a minimum of the free energy for large r, but for smaller r it describes only an extremum and is unstable to a collapse of the vortices.

To find the force that would be detected by the AFM tip as the vortices are wound around one another into an entangled state, we first consider the large r case of Eq. (4) when the entwined vortex configuration is stable. We fix the total winding angle, $\Delta\theta = \theta(L) - \theta(0)$, and the values $r(0), r(L)$. The force that the dragged vortex exerts on the AFM tip can be found by taking a derivative of the free energy with respect to r and θ. We find that the *angular* force on the top end of each vortex is $\tilde{\epsilon}_1 r\partial_z\theta(L)$, while the *radial* force on each is $\tilde{\epsilon}_1\partial_z r(L)$. The radial force will vanish when $r, \partial_z\theta$ obey Eq. (4) at the top and bottom of the sample, giving a solution with constant radius and pitch $\partial_z\theta = (\theta(L) - \theta(0))/L$. In this case, we plot the angular force as a function of pitch in Fig. 2.

Experimental Implications– The magnitude of the angular force is large enough to be detected experimentally. For example, consider two vortices in a YBCO sample. For this material, $\tilde{\epsilon}_1 \approx 5\epsilon_0$, where $\epsilon_0 \approx 140$ pN. Thus, in Fig. 2, a force of 0.1 $\tilde{\epsilon}_1$ would correspond to approximately 70 pN, a value within the range of forces detectable with AFM. In order to convert the pitch $\partial_z\theta$ plotted in Fig. 2 into the total angular displacement $\Delta\theta$ imposed on the dragged vortex, we must know the thickness L of the sample in the z direction. Assuming $L = 1\mu$m gives $\Delta\theta = L\partial_z\theta = 0.91\pi$ for $\partial_z\theta = 0.2$. The spacing of the pins at the bottom of the sample does not affect the force measured at the top of the sample unless it is of order the sample thickness or wider, due to the fact that the vortex spacing in the middle of the sample depends only on the pitch.

If the radial force is non-vanishing, then $r(z)$ is not a constant function: by applying a radial force at the top we drive the vortices away from the preferred spacing. If $r(L)$ is too large for the pitch, then $r(z)$ will decrease in the middle of the sample, while if $r(L)$ is too small, $r(z)$ will increase in the middle of the sample. Solutions to the equations of motion can be found numerically [22], as in Fig. 1. For large enough L, one finds that in the middle of the sample the $r, \partial_z\theta$ are given with good accuracy by Eq. (4), for large enough r when the equation describes a minimum.

We next consider under what conditions the twisted vortex configuration becomes unstable. This occurs when Eq. (4) no longer describes a minimum. We find by differentiating the free energy twice that for stability at fixed J, we need

$$\tilde{\epsilon}_1\frac{3J^2}{r^4} - \epsilon_0\frac{2}{\lambda^2}(K_0(2r/\lambda) + K_2(2r/\lambda)) < 0. \tag{5}$$

When Eq. (5) vanishes, at $r \approx 1.19\lambda$, the system is marginal, and for smaller r, the system is unstable to perturbations. In this case, the repulsion between the vortices is unable to overcome the elastic energy, and the two vortices will be driven together, meeting at a singularity for some z with $r(z) = 0$. Only a finite energy cost is paid to have the two vortices meet at a point, while an arbitrary amount of winding can be accomplished at that point with no free energy cost. Within an elastic string model, it can be shown that for any vortex-vortex interaction energy which diverges less strongly than $1/r^2$ there is an instability of this nature for sufficiently small r. At the marginal $r \approx 1.19\lambda$, the angular force on each vortex is equal to $(0.45...)\sqrt{\tilde{\epsilon}_1\epsilon_0}$. Thus, this is the largest angular force possible in this experimental setup, while the minimum stable vortex spacing is $2r \approx 2.39\lambda$.

In more highly anisotropic materials such as BSCCO, the elastic string model for the vortex lines is expected to break down due to the possibility of decoupling of vortex pancakes on adjacent layers. Consider a magnetic AFM tip bound to a pancake at the top of a vortex line in BSCCO. If this pancake decouples from the rest of the vortex line below, then the angular force as a function of angular displacement will not follow the form shown in Fig 2. but will instead be periodic in the winding angle, due to the interaction with the remaining stack of pancake vortices left behind. This is illustrated by a simulation of a pancake vortex system [23] shown in Fig. 3. The force from a single pancake is extremely

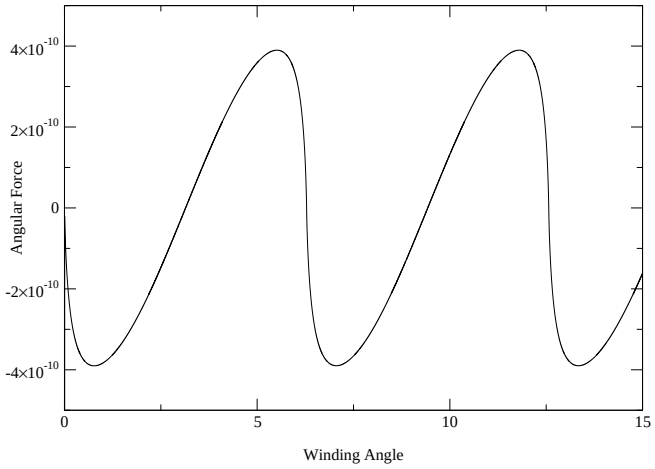

FIG. 3. Angular force on a decoupled pancake vortex in units of $\tilde{\epsilon}_1$ as a function of total winding angle $\Delta\theta$, obtained from a simulation of pancake vortices.

small, of order 10^{-20}N; thus it is natural to ask how to experimentally determine whether one pancake is attached to the AFM tip, or whether the entire vortex stack has detached from the AFM tip so that the tip is moving freely over the sample. The presence of a vortex under the AFM tip can be detected by means of a local density of states measurement performed by temporarily changing the mode of operation of the tip to a tunneling probe.

Discussion— The local experimental probe that we propose can also be used to explore numerous other properties of the vortex system besides vortex entanglement. For example, in a geometry containing only one magnetic pin and one vortex line, the AFM tip can be used to measure the vortex line tension directly. If the line tension is known, the tip could be used to tear a vortex away from a (weaker) individual pin, such as a grain boundary, and the pinning force could be measured. By applying a transport current to the sample, the Lorentz force can be determined directly. Local rheology measurements are also possible in the vortex lattice state; for example, the local elastic constants can be probed by moving a single vortex back and forth around its lattice equilibrium position. The temperature dependence of both the elastic constants and the pinning energy could also be probed.

Conclusion— We have proposed an experimental setup for constructing and probing entangled states of superconducting vortices, and shown that the forces associated with vortex entanglement are experimentally measurable. This kind of experimental setup can be generalized to other types of vortices, as in fluid turbulence. Within the elastic string model, we find that the entangled state is only stable up to a maximum pitch or minimum vortex spacing. The instabilities we have found raise the question of whether the entangled state can exist with a high density of vortices. To answer this question and to compare pancake and elastic string models, an experimental test of our proposal is desirable.

Acknowledgments— We thank C. Reichhardt for helpful discussions. This work was supported by DOE grant W-7405-ENG-36.

[1] G. Blatter *et al.,* Rev. Mod. Phys. **66**, 1125 (1994).
[2] D.R. Nelson, Phys. Rev. Lett. **60**, 1973 (1988).
[3] D.R. Nelson and H.S. Seung, Phys. Rev. B **39**, 9153 (1989).
[4] M.C. Marchetti and D.R. Nelson, Phys. Rev. B **42**, 9938 (1990).
[5] S.P. Obukhov and M. Rubinstein, Phys. Rev. Lett. **65**, 1279 (1990).
[6] J.R. Clem, Phys. Rev. B **26**, 2463 (1982).
[7] M.C. Marchetti, J. Appl. Phys. **69**, 5185 (1991).
[8] A. Sudbø and E.H. Brandt, Phys. Rev. Lett. **67**, 3176 (1991).
[9] M.A. Moore and N.K. Wilkin, Phys. Rev. B **50**, 10294 (1994); M.J.W. Dodgson and M.A. Moore, *ibid.* **51**, 11887 (1995); A. Schönenberger, V. Geshkenbein, and G. Blatter, Phys. Rev. Lett. **75**, 1380 (1995). M. Bou-Diab, M.J.W. Dodgson, and G. Blatter, *ibid.* **86**, 5132 (2001).
[10] C. Carraro and D.S. Fisher, Phys. Rev. B **51**, 534 (1995).
[11] D. Domínguez, N. Grønbech-Jensen, and A.R. Bishop, Phys. Rev. Lett. **75**, 4670 (1995); H. Nordborg and G. Blatter, *ibid.* **79**, 1925 (1997); E.A. Jagla and C.A. Balseiro, Phys. Rev. B **55**, 3192 (1997); S. Ryu and D. Stroud, *ibid.* **57**, 14476 (1998); H. Nordborg and G. Blatter, *ibid.* **58**, 14556 (1998); A. van Otterlo, R.T. Scalettar, and G.T. Zimányi, Phys. Rev. Lett. **81**, 1497 (1998); Y. Nonomura, X. Hu, and M. Tachiki, Phys. Rev. B **59**, R11657 (1999); J. Lidmar and M. Wallin, *ibid.* **59**, 8451 (1999); A.M. Ettouhami, *ibid.* **65**, 134504 (2002).
[12] Y-H. Li and S. Teitel, Phys. Rev. B **49**, 4136 (1994).
[13] X. Hu, S. Miyashita, and M. Tachiki, Phys. Rev. Lett. **79**, 3498 (1997); S. Ryu and D. Stroud, *ibid.* **78**, 4629 (1997); T. Chen and S. Teitel, Phys. Rev. B **55**, 15197, 11766 (1997); T.J. Hagenaars *et al.*, *ibid.* **55**, 11706 (1997); X. Hu, S. Miyashita, and M. Tachiki, *ibid.* **58**, 3438 (1998); A.K. Nguyen and A. Sudbø, *ibid.* **57**, 3123 (1998); **60**, 15307 (1999).
[14] A. Sudbø and E.H. Brandt, Phys. Rev. B **43**, 10482 (1991).
[15] P. Benetatos and M.C. Marchetti, Phys. Rev. B **59**, 6499 (1999); Physica C **332**, 237 (2000).
[16] D. López *et al.*, Phys. Rev. Lett. **80**, 1070 (1998); T. Puig and X. Obradors, *ibid.* **84**, 1571 (2000).
[17] X.G. Qiu *et al.*, Phys. Rev. B **58**, 8826 (1998).
[18] L. Miu *et al.*, Phys. Rev. B **57**, 3151 (1998).
[19] S.A. Grigera *et al.*, Physica C **371**, 237 (2002).
[20] D.R. Nelson, Nature **375**, 356 (1995); D. Ertas and D.R. Nelson, Physica C **272**, 79 (1996).
[21] J.I. Martín *et al.*, Phys. Rev. Lett. **79**, 1929 (1997); D.J. Morgan and J.B. Ketterson, *ibid.* **80**, 3614 (1998).
[22] To find such solutions, one can use a shooting technique. It is useful also to exploit the conservation law: $\tilde{\epsilon}_1[J^2/r^2 + (\partial_z r)^2] - (2\epsilon_0)K_0(2r/\lambda) = \text{const.}$
[23] C.J. Olson *et al.*, Phys. Rev. Lett. **85**, 5416 (2000).